J|A|C|S
ARTICLES
Published on Web 03/06/2004

Solid-Phase Synthesis of Positively Charged Deoxynucleic Guanidine (DNG) Tethering a Hoechst 33258 Analogue: Triplex and Duplex Stabilization by Simultaneous Minor Groove Binding

Putta Mallikarjuna Reddy and Thomas C. Bruice*

Contribution from the Department of Chemistry and Biochemistry, University of California at Santa Barbara, Santa Barbara, California 93106

Received December 5, 2003; E-mail: tcbruice@bioorganic.ucsb.edu

Abstract: Deoxynucleic guanidine (DNG), a DNA analogue in which positively charged guanidine replaces the phosphodiester linkages, tethering to Hoechst 33258 fluorophore by varying lengths has been synthesized. A pentameric thymidine DNG was synthesized on solid phase in the 3′ → 5′ direction that allowed stepwise incorporation of straight chain amino acid linkers and a bis-benzimidazole (Hoechst 33258) ligand at the 5′-terminus using PyBOP/HOBt chemistry. The stability of $(DNA)_2$·DNG−H triplexes and DNA·DNG−H duplexes formed by DNG and DNG−Hoechst 33258 (DNG−H) conjugates with 30-mer double-strand (ds) DNA, d(CGCCGCGCGCGCGAAAAACCCGGCGCGCGC)/d(GCGGCGCGCGCGCTTTTTGGGC-CGCGCGCG), and single-strand (ss) DNA, 5′-CGCCGCGCGCGCGAAAAACCCGGCGCGCGC-3′, respectively, has been evaluated by thermal melting and fluorescence emission experiments. The presence of tethered Hoechst ligand in the 5′-terminus of the DNG enhances the $(DNA)_2$·DNG−H triplex stability by a ΔT_m of 13 °C. The fluorescence emission studies of $(DNA)_2$·DNG−H triplex complexes show that the DNG moiety of the conjugates bind in the major groove while the Hoechst ligand resides in the A:T rich minor groove of dsDNA. A single G:C base pair mismatch in the target site decreases the $(DNA)_2$·DNG triplex stability by 11 °C, whereas $(DNA)_2$·DNG−H triplex stability was decreased by 23 °C. Inversion of A:T base pair into T:A base pair in the center of the binding site, which provides a mismatch selectively for DNG moiety, decreases the triplex stability by only 5−6 °C. Upon hybridization of DNG−Hoechst conjugates with the 30-mer ssDNA, the DNA·DNG−H duplex exhibited significant increase in the fluorescence emission due to the binding of the tethered Hoechst ligand in the generated DNA·DNG minor groove, and the duplex stability was enhanced by ΔT_m of 7 °C. The stability of $(DNA)_2$·DNG triplexes and DNA·DNG duplexes is independent of pH, whereas the stability of $(DNA)_2$·DNG−H triplexes decreases with increase in pH.

Introduction

Sequence-specific targeting of ss and ds/DNA using duplex- and triplex-forming oligonucleotides offers a promising antisense/antigene strategy to control the regulation of gene expression,[1] site-directed mutagenesis,[2] and gene repair.[3,4] Although the DNA oligonucleotides bind with high specificity, the triplex complexes formed are thermodynamically less stable than the duplex complexes. This is partially due to the charge repulsion resulting from bringing together the three polyanionic DNA strands. Therefore, the ideal antisense/antigene agents should have high affinity for DNA while still maintaining fidelity of recognition, stability toward nucleases, and efficient membrane permeability. To enhance the affinity of the duplex- and triplex-forming oligonucleotide sequences for the target ss/dsDNA sequences under physiological conditions, various approaches have been taken to develop novel chemically modified nucleotides.[5] One approach is the incorporation of neutral internucleoside linkages that eliminate mutual repulsions between the negatively charged phosphodiester backbones.[6−10]

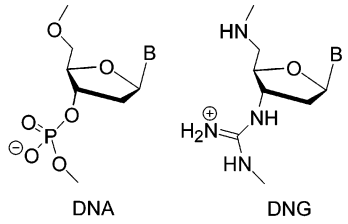

Figure 1. Chemical structures of DNA and DNG.

(1) (a) Giovannangeli, C.; Helene, C. *Antisense Nucleic Acid Drug Dev.* **1997**, *7*, 413. (b) Giovannangeli, C.; Perrouault, L.; Escude, C.; Thuong, N.; Helene, C. *Biochemistry* **1996**, *35*, 10539. (c) Maher, L. J.; Dervan, P. B.; Wold, B. *Biochemistry* **1992**, *31*, 70.
(2) (a) Wang, G.; Levy, D. D.; Seidman, M. M.; Glazer, P. M. *Mol. Cell. Biol.* **1995**, *15*, 1759. (b) Wang, G.; Seidman, M. M.; Glazer, P. M. *Science* **1996**, *271*, 802.
(3) Broitman, S.; Amosova, O.; Dolinnaya, N. G.; Fresco, J. R. *J. Biol. Chem.* **1999**, *274*, 21763.
(4) Johnson, M. D., III; Fresco, J. R. *Chromosoma* **1999**, *108*, 181.
(5) (a) Uhlmann, E.; Peyman, A. *Chem. Rev.* **1990**, *90*, 543. (b) Milligan, J. F.; Matteucci, M. D.; Martin, J. C. *J. Med. Chem.* **1993**, *36*, 1923. (c) Kurreck, J. *Eur. J. Biochem.* **2003**, *270*, 1628.
(6) De Mesmaeker, A.; Waldener, A.; Lebreton, J.; Hoffmann, P.; Fritsch, V.; Wolf, R. M.; Freier, S. M. *Angew. Chem., Int. Ed. Engl.* **1994**, *33*, 226.
(7) Levis, J. T.; Butler, W. O.; Tseng, B. Y.; Ts'o, P. O. P. *Antisense Res. Dev.* **1995**, *5*, 251.

10.1021/ja031557s CCC: $27.50

Another approach is to replace the entire phosphodiester backbone, such as in the cases of peptide nucleic acid (PNA),[11] phosphonic ester nucleic acids (PHONA),[12] and nucleic acid analogue peptide (NAAP).[13] Recent studies have shown that the introduction of positively charged groups at multiple sites in the backbone,[14,15] sugar,[16] or base[17] can produce stable duplexes and triplexes.[18] Our approach is to replace the phosphodiester linkages with positively charged achiral guanidinium groups. Incorporation of positively charged guanidinium groups (Figure 1) in the place of negatively charged phosphodiester linkages greatly enhances the oligonucleotide complex stability through charge−charge interactions.[19]

A number of well-characterized small molecule ligands such as intercalators,[20] polyamines,[21] polyamides,[22] and fluorescent dyes[23] are known to interact with duplex and triplex DNA and enhance stability by providing additional interactions. Conjugation of these ligands to duplex- and triplex-forming oligonucleotides exhibited further enhanced stability of the duplex and triplex complexes.[24] Among these ligands, the bis-benzimidazole derivatives bind with high affinity in the minor groove of double-stranded B-DNA with a strong preference for A:T base pairs. This binding results in enhanced helix stabilization and also a tremendous enhancement in the observed fluorescence emission of the ligand.[25] These fluorescence properties have been useful in a variety of applications such as determination of A:T base pair content in DNA samples,[26] determination of cell numbers,[27] and chromosomal sorting.[28] The best-known compound in the bis-benzimidazole family, the Hoechst 33258 dye's assay sensitivity is approximately 1 ng/mL, and the quantum yield effects are sensitive enough to detect one target cell in a million mixed cell population.[29] Furthermore, the Hoechst 33258 dye is capable of crossing the cellular and nuclear membranes and stain as fluorescent DNA and chromosomes.[28] We have recently taken advantage of these characteristics of Hoechst 33258 ligand and developed novel tripyrrole−Hoechst conjugates.[30] These conjugates are capable of passing through NIH 3T3 cell membrane and inhibit a DNA−TF complex formation by binding to its nuclear DNA targets.[31]

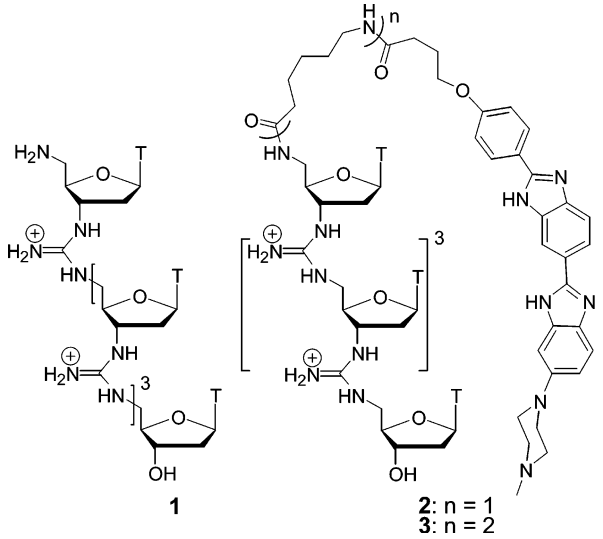

Figure 2. Pentameric thymidyl DNG and Hoechst 33258-tethered DNGs.

Although the DNA oligonucleotides conjugated to minor groove binding ligands exhibited increased duplex and triplex stability,[22,23] the oligonucleotides must be of a reasonable length to form stable duplexes and triplexes. We have recently shown that a short sequence of DNG having positively charged guanidinium backbone can form stable complexes by electrostatic attractions.[19] Additionally, the guanidinium linkages are resistant to nucleases,[32] and also the positive charges of the backbone may give rise to cell membrane permeability through electrostatic attraction of the oligonucleotide to the negatively charged phosphates of the cell surface. Complex stabilization by groove binding as well as membrane permeability of Hoechst derivatives suggests that tethering a fluorophore such as Hoechst

(8) Waldener, A.; De Mesmaeker, A.; Lebreton, J.; Fritsch, V.; Wolf, R. M. *Synlett* **1994**, 57.
(9) Morvan, F.; Sanghvi, Y. S.; Perbost, M.; Vasseur, J.-J.; Bellon. L. *J. Am. Chem. Soc.* **1996**, *118*, 255.
(10) Wang, J.; Matteucci, M. D. *Bioorg. Med. Chem. Lett.* **1997**, *7*, 229.
(11) (a) Nielsen, P. E. *Pure Appl. Chem.* **1998**, *70*, 105. (b) Uhlmann, E.; Peyman, A.; Breipohl, G.; Will, D. W. *Angew. Chem., Int. Ed.* **1998**, *37*, 2796.
(12) Peyman, A.; Uhlmann, E.; Wagner, K.; Augustin, S.; Breipohl, G.; Will, D. W.; Schafer, A.; Wallmeier, H. *Angew. Chem., Int. Ed. Engl.* **1996**, *35*, 2636.
(13) Fujii, M.; Yoshida, K.; Hidaka, J. *Bioorg. Med. Chem. Lett.* **1997**, *7*, 637.
(14) Michel, T.; Debart, F.; Vasseur, J.-J. *Tetrahedron Lett.* **2003**, *44*, 6579.
(15) (a) Skibo, E. B.; Xing, C. *Biochemistry* **1998**, *37*, 15199. (b) Chaturvedi, S.; Horn, T.; Letsinger, R. L. *Nucleic Acids Res.* **1996**, *24*, 2318. (c) Letsinger, R. L.; Singman, C. N.; Histand, G.; Salunkhe, M. *J. Am. Chem. Soc.* **1988**, *110*, 4470.
(16) Hichman, D. T.; Tan, T. H. S.; Morral, J.; King, P. M.; Cooper, M. A.; Micklefield, J. *Org. Biomol. Chem.* **2003**, *1*, 3277.
(17) Ueno, Y.; Mikawa, M.; Matsuda, A. *Bioconjugate Chem.* **1998**, *9*, 33.
(18) For review see: Fox, K. R. *Curr. Med. Chem.* **2000**, *7*, 17.
(19) (a) Reddy, P. M.; Bruice, T. C. *Bioorg. Med. Chem. Lett.* **2003**, *13*, 1281. (b) Linkletter, B. A.; Szabo, I. E.; Bruice, T. C. *Nucleic Acid Res.* **2001**, *29*, 2370. (c) Linkletter, B. A.; Szabo, I. E.; Bruice, T. C. *J. Am. Chem. Soc.* **1999**, *121*, 3888. (d) Browne, K. A.; Dempcy, R. O.; Bruice, T. C. *Proc. Natl. Acad. Sci. U.S.A.* **1995**, *92*, 7051. (e) Dempcy, R. O.; Browne, K. A.; Bruice, T. C. *Proc. Natl. Acad. Sci. U.S.A.* **1995**, *92*, 6097. (f) Dempcy, R. O.; Browne, K. A.; Bruice, T. C. *J. Am. Chem. Soc.* **1995**, *117*, 6140.
(20) Thoung, N. T.; Asseline, U.; Moneney-Garestier, T. In *Oligonucleotides. Anti-Sense Inhibitors of Gene Expression;* Cohen, J. S., Ed.; CRC Press: Boca Raton, FL, 1989; pp 25−52.
(21) Lemaitre, M.; Bayard, B.; Lebleu, B. *Proc. Natl. Acad. Sci. U.S.A.* **1987**, *84*, 648.
(22) (a) Szewczyk, J.; Baird, E. E.; Dervan, P. B. *Angew. Chem., Int. Ed. Engl.* **1996**, *35*, 1487. (b) Sinyakov, A. N.; Lokhov, S. G.; Kutyavin, I. V.; Gamper, H. B.; Meyer, R. B. *J. Am. Chem. Soc.* **1995**, *117*, 4995.
(23) (a) Robles, J.; Rajur, S. B.; McLaughlin, L. W. *J. Am. Chem. Soc.* **1996**, *118*, 5820. (b) Wiederholt, K.; Rajur, S. B.; Giuliano, J., Jr.; O'Donnell, M. J.; McLaughlin, L. W. *J. Am. Chem. Soc.* **1996**, *118*, 7055. (c) Robles, J.; McLaughlin, L. W. *J. Am. Chem. Soc.* **1997**, *119*, 6014. (d) Rajur, S. B.; Robles, J.; Wiederholt, K.; Kuimelis, R. G.; McLaughlin, L. W. *J. Org. Chem.* **1997**, *62*, 523.
(24) Helix-stabilizing ligands: (a) Mergny, J. L.; Duval-Valentin, G.; Nguyen, C. H.; Perrouault, L.; Faucon, B.; Rougee, M.; Montenay-Garestier, T.; Bisagni, E.; Helene C. *Science* **1992**, *256*, 1681. (b) Lee, J. S.; Latimer, L. J. P.; Hampel, K. J. *Biochemistry* **1993**, *32*, 5591. (c) Wilson, W. D.; Tanious, F. A.; Mizan, S.; Yao, S.; Kiselyov, A. S.; Zon, A. S.; Strekowski, G. L. *Biochemistry* **1993**, *32*, 10614. (d) Fox, K. R.; Polucci, P.; Jenkins, T. C.; Neidle, S. *Proc. Natl. Acad. Sci. U.S.A.* **1995**, *92*, 7887. (e) Escude, C.; Nguyen, C. H.; Kukreti, S.; Janin, Y.; Sun, J. S.; Bisagni, E.; Garestier T.; Helene, C. *Proc. Natl. Acad. Sci. U.S.A.* **1998**, *95*, 3591.
(25) (a) Zimmer, C.; Wahnert, U. *Prog. Biophys. Mol. Biol.* **1986**, *47*, 31. (b) Lootiens, F. G.; Regenfuss, P.; Zechel, A.; Dumortier, L.; Clegg, R. M. *Biochemistry* **1990**, *29*, 9029.
(26) (a) Weisblum, B.; Haenssler, E. *Chromosoma* **1974**, *46*, 255. (b) Coming, D. E. *Chromosoma* **1975**, *52*, 229. (c) Sterzel, W.; Bedford, P.; Eisenbrand, G. *Anal. Biochem.* **1985**, *147*, 462. (d) Araki, T.; Yamamoto, A.; Yamada, M. *Histochemistry* **1987**, *87*, 331. (e) Karawajew, L.; Rudchenko, S.; Wlasik, T.; Trakht, I. *J. Immunol. Methods* **1990**, *129*, 277.
(27) (a) Downs, T. R.; Wilfinger, W. W. *Anal. Biochem.* **1983**, *131*, 538. (b) Adams, C. J.; Storrie, B. *Histochem. Cytochem.* **1981**, *29*, 326.
(28) (a) Holmquist, G. *Chromosoma* **1975**, *49*, 333. (b) Arndt-Jovin, D. J.; Jovin, T. M. *Cytometry* **1990**, *11*, 80. (c) Frau, S.; Bernadou, J.; Meunier, B. *Bull. Soc. Chim. Fr.* **1996**, *133*, 1053.
(29) Lee, B. R.; Haseman, D. B.; Reynolds, C. P. *Cytometry* **1989**, *10*, 256.
(30) (a) Satz, A. L.; Bruice, T. C. *J. Am. Chem. Soc.* **2001**, *123*, 2469. (b) Satz, A. L.; Bruice, T. C. *Bioorg. Med. Chem.* **2002**, *10*, 241. (c) Reddy, P. M.; Jindra, P. T.; Satz, A. L.; Bruice, T. C. *J. Am. Chem. Soc.* **2003**, *125*, 7843.
(31) (a) White, C. M.; Satz, A. L.; Bruice, T. C.; Beerman, T. A. *Proc. Natl. Acad. Sci. U.S.A.* **2001**, *98*, 10590. (b) White, C. M.; Satz, A. L.; Gawron, L. S.; Bruice, T. C.; Beerman, T. A. *Biochim. Biophys. Acta* **2001**, *1574*, 100.
(32) Barawkar, D. A.; Bruice, T. C. *Proc. Natl. Acad. Sci. U.S.A.* **1998**, *95*, 11047.

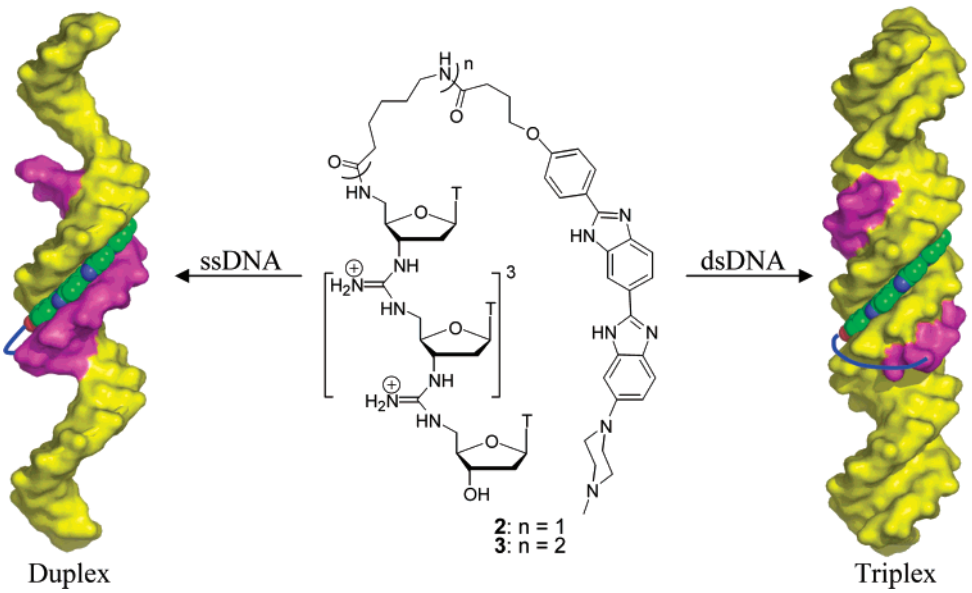

Figure 3. Proposed models for DNA·DNG−H duplex and $(DNA)_2$·DNG−H triplex complexes formed by DNA and DNG−Hoechst 33258 conjugates. The ssDNA and dsDNA are represented in yellow, DNG is represented in magenta, Hoechst dye is represented in spheres, and the linker is represented in blue.

33258 to the 5′-terminus of the positively charged DNG could further enhance the stability of DNA·DNG duplex and $(DNA)_2$·DNG triplex complexes by simultaneous minor groove binding. Furthermore, these DNG−Hoechst conjugates might be better able to cross the cellular and nuclear membranes than the unconjugated DNG sequences and bind to its nuclear DNA targets. More importantly, these conjugates, which would grasp dsDNA through both major and minor groove binding, are also promising for development of transcription factor inhibitors.[31,33] In this study, we describe the synthesis of the modified monomers for the DNG solid-phase synthesis (SPS) and the Hoechst 33258 derivative containing a linker that allows covalent attachment to the 5′-terminus of the DNG sequence. We report on the covalent conjugation of such agents to DNG, the duplex and triplex stabilization, and the fluorescent properties resulting from simultaneous minor groove binding of these DNG−Hoechst 33258 conjugates (**1**−**3**, Figure 2).

Results and Discussion

In the antisense technology for controlling translation, a designed oligonucleotide binds sequence-specifically to the mRNA by Watson−Crick hydrogen bonds.[5] Antisense oligonucleotide sequences generate a minor groove similar to dsDNA upon hybridization to the complementary target sequence. On the other hand, in the antigene technology for controlling gene transcription, a designed oligonucleotide binds to the major groove of the dsDNA by Hoogsteen or reverse Hoogsteen hydrogen bonds and forms a local triple helix.[34] In DNA triplex, in which the third strand occupies the major groove, the minor groove remains largely unencumbered. A variety of studies have shown that tethering a minor groove binding ligand such as Hoechst 33258 or polyamides to the 5′-terminus of the duplex- and triplex-forming strand enhances the duplex and triplex stability by binding simultaneously in the minor groove.[22,23] On the basis of these results and the strong affinity of DNG toward target DNA, we envisaged the possibility that tethering a bis-benzimidazole ligand to the polycationic DNG strand could greatly increase the already strong binding of DNG to DNA. DNG−Hoechst 33258 conjugates should bind sequence-specifically to a dsDNA target site to form a local $(DNA)_2$·DNG−H triplex in which the DNG strand would be located in the major groove and the Hoechst ligand would occupy the minor groove of the target duplex (Figure 3). On the other hand, the same DNG−Hoechst conjugates can also form stable DNA·DNG−H duplexes by binding sequence-specifically to the targeted ssDNA. The tethered Hoechst moiety can further stabilize the DNA/DNG duplex by folding back into the generated minor groove, thereby providing additional binding interactions (Figure 3). For a $(DNA)_2$·DNG−H triplex to benefit from both modes of binding, the linker used for tethering the ligand to the DNG sequence must be long enough to reach the minor groove from the 5′-terminus of the DNG third strand in the major groove by traversing the phosphoribose backbone. However, in the case of DNA·DNG−H duplex, a shorter linker may suffice to fold back and permit the tethered ligand to reach the minor groove of DNA·DNG duplex. Also, the minor groove of DNA·DNG duplex will not be the same as that of DNA·DNA duplex.[35] To evaluate these considerations, we have synthesized DNG−Hoechst 33258 conjugates with 11 and 18 atom linkers (compounds **2** and **3** respectively).

The synthetic strategy we have developed for the DNG SPS involves the coupling of 3′-Fmoc-protected thiourea in the presence of $HgCl_2$/TEA with the corresponding 5′-NH_2 of the growing oligo chain on long chain alkylamine-derivatized controlled pore glass (CPG).[19a,b] The DNG−Hoechst 33258 conjugates (**2** and **3**) were also synthesized on solid phase by stepwise incorporation of an amino acid straight chain linker and a Hoechst acid into the 5′-NH_2 of the DNG using PyBOP/HOBt chemistry. To facilitate the stepwise synthesis of DNG and DNG−Hoechst conjugates, the required monomers **4**, **8**, **10**, and **15** were synthesized as described in Schemes 1−4 .

Synthesis of Monomers. The loading monomer, 5′-monomethoxytritylamino-2′,5′-dideoxythymidine was synthesized

(33) Arya, D. P.; Willis, B. *J. Am. Chem. Soc.* **2003**, *125*, 12398.
(34) Thuong, N. T.; Helene, C. *Angew. Chem., Int. Ed. Engl.* **1993**, *32*, 666.
(35) Luo, J.; Bruice, T. C. *J. Am. Chem. Soc.* **1998**, *120*, 1115.

Scheme 1. CPG Loaded 5′-Modified Monomer

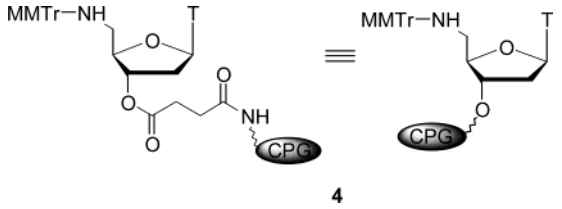

4

Scheme 2 [a]

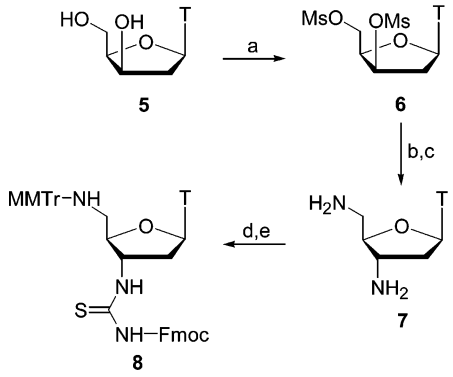

[a] Reagents and conditions: (a) CH_3SO_2Cl 5.0 equiv, pyridine, 0 °C. Room temperature, overnight. (b) LiN_3 20.0 equiv, DMF, 80 °C, 4 h. (c) 10% Pd/C, H_2, EtOH, 2 h. (d) MMTrCl 1.0 equiv, TEA 2.0 equiv, DCM, 2 h. (e) Fmoc-NCS, 1.2 equiv, DCM, room temperature, 2 h.

Scheme 3 [a]

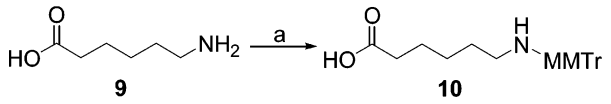

9 **10**

[a] Reagents and conditions: (a) MMTrCl 1.2 equiv, pyridine, room temperature, 6 h.

Scheme 4 [a]

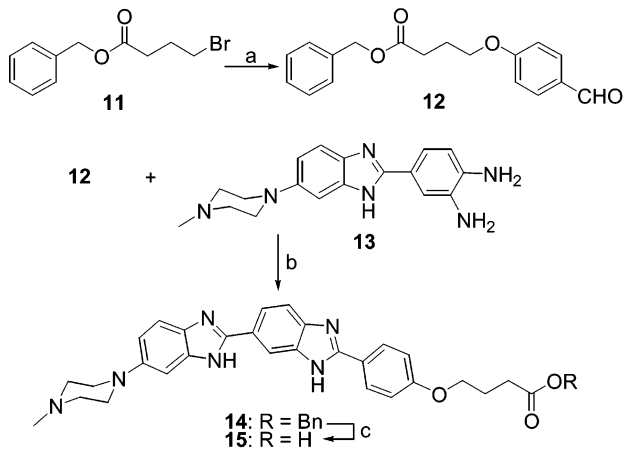

[a] Reagents and conditions: (a) 4-hydroxybenzaldehyde, Cs_2CO_3, anhydrous DMA, 100 °C, 15 h. (b) Nitrobenzene, 130 °C, 24 h. (c) 10% Pd/C, H_2, EtOH, 4 h.

from 5′-amino-2′-deoxythymidine[36] and loaded on to the CPG solid support via succinyl linker (Scheme 1) to afford the CPG-derivatized monomer **4**[19a] (see Supporting Information). The unreacted CPG amine sites were covered by capping with acetic anhydride/TEA, and then the 5′-MMTr was deprotected with 3% DCA in DCM solution. The loading yield, 39.6 μmol/g, was determined spectrophotometrically from the amount of MMTr cation released.

The 3′,5′-diamino protected thymidyl building block **8**, required for the coupling reaction to make the guanidinium backbone, was accomplished from 3′-OH inverted **5**[19a,37] (Scheme 2). The 3′-OH inverted thymidine **5** was readily converted into 3′,5′-dimesyl derivative **6** in quantitative yield by reacting with mesyl chloride in pyridine. Treatment of **6** with LiN_3 in DMF at 80 °C resulted in its 3′,5′-diazido derivative, which on further reduction with 10% Pd/C gave 3′,5′-diamino-2′,3′,5′-trideoxythymidine **7**.[19a,38] Selective protection of 5′- and 3′-NH_2 groups of **7** with acid-labile MMTr and base-cleavable Fmoc groups gave **8**. Initially, the 5′-NH_2 was selectively protected by reacting with 1 equiv of MMTrCl in the presence of TEA, and then the 3′-NH_2 was protected by the addition of Fmoc-NCS[39] to afford the desired coupling monomer **8** (Scheme 2).

To achieve the stepwise synthesis of DNG−Hoechst conjugates with different linker lengths, we chose **10** and **15** as building blocks (Schemes 3 and 4). The 6-monomethoxytritylamino-hexanoic acid (**10**) was prepared easily, in ~95% yield,[40] through the reaction of commercially available 6-aminohexanoic acid (**9**) with MMTrCl in dry pyridine (Scheme 3). The Hoechst acid **15** was synthesized as described in Scheme 4. Benzyl 4-(4-formylphenoxy)butanoate (**12**) was synthesized in 98% yield from benzyl 4-bromobutyrate[41] (**11**) by reacting with 4-hydroxybenzaldehyde in the presence of Cs_2CO_3 in *N*,*N*-dimethylacetamide (DMA). Condensation of **12** with *ortho*-diamine **13**[42] in nitrobenzene at 130 °C gave benzyl ester of Hoechst acid **14** in 87% yield. Further, hydrogenation at 50 psi using 10% Pd/C conveniently afforded **15** in quantitative yield.

DNG (1) Solid-Phase Synthesis. The pentameric thymidyl DNG **1** was synthesized in a stepwise manner on solid-phase using CPG-derivatized **4** and 3′,5′-protected monomer **8** (Scheme 5). The synthesis proceeds in a 3′ → 5′ direction that is compatible with the cleavage conditions used in the DNA SPS. Coupling of **8** with MMTr deprotected **4** for the formation of the guanidinium linkage was accomplished in the presence of $HgCl_2$ and TEA. Treatment of **8** with $HgCl_2$ in the presence of TEA converts the 3′-Fmoc-protected thiourea into an intermediate carbodiimide,[19a,b] which reacts in situ with the 5′-NH_2 of CPG-loaded monomer to provide an Fmoc-protected guanidinium linkage (Scheme 5). This Fmoc protecting group remains in place on the guanidinium linkage until the end of the SPS when it is readily removed during cleavage of the oligomer from the CPG. The unreacted 5′-NH_2 sites were blocked by capping reaction, rendering them inert toward further chain extension. The terminal 5′-MMTr group was removed, and the coupling yield for this step was 99% as determined by UV absorbance of the released MMTr cation. The whole coupling cycle (coupling/capping/deprotection) was repeated three more times

(36) Horwitz, J. P.; Tomson, A. J.; Urbanski, J. A.; Chua, J. *J. Org. Chem.* **1962**, *27*, 3045.
(37) Pathak, A. K.; Pathak, V.; Seitz, L. E.; Tiwari, K. N.; Akhtar, M. S.; Reynolds, R. C. *Tetrahedron Lett.* **2001**, *42*, 7755.
(38) Herdewijn, P.; Balzarini, J.; Pauwels, R.; Janssen, G.; Van Aerschot, A.; De Clercq, E. *Nucleosides Nucleotides* **1989**, *8*, 1231.
(39) Kearney, P. C.; Fernandez, M.; Flygare, J. A. *J. Org. Chem.* **1998**, *63*, 196.
(40) Berube, G.; Richardson, V. J.; Ford, C. H. J. *Synth. Commun.* **1991**, *21*, 931.
(41) Baba, A.; Kawamura, N.; Makino, H.; Ohta, Y.; Taketomi, S.; Sohda, T. *J. Med. Chem.* **1996**, *39*, 5176.
(42) (a) Sadat Ebrahimi, S. E.; Bibby, M. C.; Fox, K. R.; Douglas, K. T. *Anti-Cancer Drug Des.* **1995**, *10*, 463. (b) Argentini, M.; Dos Santos, D. F.; Weinreich, R.; Hansen, H.-J. *Inorg. Chem.* **1998**, *37*, 6018.

Scheme 5. Solid-Phase Synthetic Scheme for Pentameric Thymidyl DNG[a]

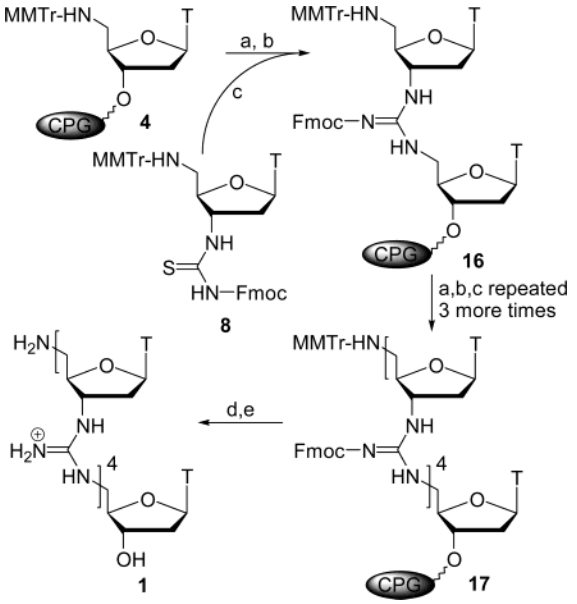

[a] Reagents and conditions: (a) Capping: $(CH_3CO)_2O$, TEA, DMF, 10 min. (b) Deprotection: 3% DCA in DCM, 1 min. (c) Coupling: monomer **8**, $HgCl_2$, TEA, DMF, 2 h, then 20% PhSH in DMF, 1 min. (d) Methanolic ammonia, room temperature, 2 h. (e) 3% DCA in DCM, 1 min.

with **8** to afford the desired DNG pentamer **17**. The coupling yield in each cycle was 95−99%, and the overall yield of the 5′-MMTr-protected oligomer was therefore expected to be ∼85%. The DNG pentamer was cleaved from CPG using a methanolic ammonia solution. The Fmoc protection on guanidinium linkages was also removed in the same step. The crude "trityl on" product was purified on reverse-phase HPLC (C_8 column) using solvent A (0.1 M TEAA buffer, pH 7.0) and a gradient of solvent B (acetonitrile) 5% → 80% in 30 min. ESI/TOF+ analysis of MMTr-protected **1** exhibited desired peaks at *m*/*z* 787.87 (M + 2H) and 525.58 (M + 3H); calcd 787.85 (M + 2H) and 525.56 (M + 3H) for $C_{74}H_{91}N_{23}O_{17}$. The 5′-MMTr of oligomer was deprotected with 3% DCA in DCM solution and precipitated with excess of ether. The precipitated product was collected by centrifugation, and analysis by RP-HPLC using the same column and solvent system revealed single peak for **1**. ESI/TOF+ analysis exhibited expected peaks at *m*/*z* 1302.72 (M + H) and 651.85 (M + 2H); calcd 1302.58 (M + H) and 651.79 (M + 2H) for $C_{54}H_{75}N_{23}O_{16}$.

Synthesis of DNG−Hoechst Conjugates 2 and 3. The novel DNG−Hoechst conjugates **2** and **3** were synthesized on solid-phase by stepwise addition of **10** and **15** to the 5′-terminus of the thymidyl pentamer **17** using PyBOP/HOBt chemistry (Scheme 6). After capping any unreacted 5′-NH_2 sites of **17**, the 5′-MMTr was removed to facilitate attachment of the amino acid straight chain linker through amide bond formation. The coupling reaction of **10** with MMTr-removed **17** was accomplished in the presence of PyBOP, HOBt, and DIPEA in DMF to afford **18**. Unreacted sites were capped with acetic anhydride/TEA, and then the MMTr substituent was removed using 3% DCA in DCM. The removal of MMTr on linker took a little longer than that of the 5′-MMTr of oligomer. The beads were treated with DCA solution for 1 min, filtered off, and washed with DCM, and the DCA treatment was repeated twice more. This procedure completely removes the MMTr moiety.

Scheme 6. Solid-Phase Synthetic Scheme for DNG−Hoechst Conjugates[a]

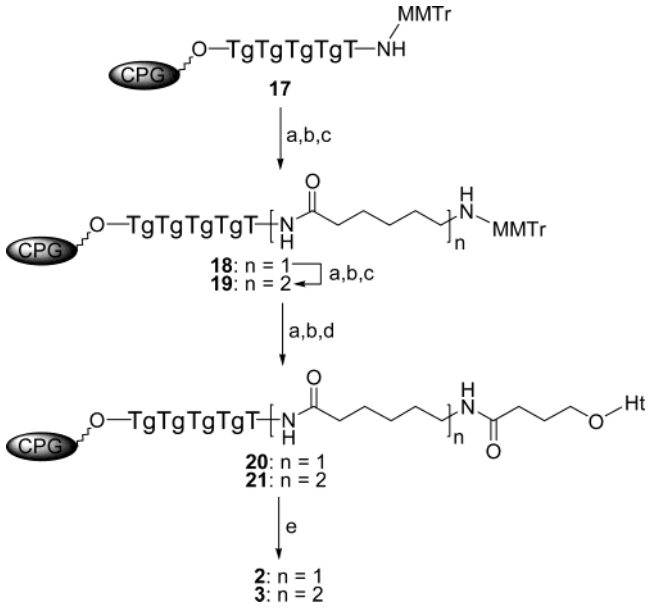

[a] Reagents and conditions: (a) Capping: $(CH_3CO)_2O$, TEA, DMF, 10 min. (b) Deprotection: 3% DCA in DCM, 1 min. (c) Coupling: monomer **10**, PyBOP, HOBt, DIPEA, DMF, 12 h. (d) Ht acid **15**, PyBOP, HOBt, DIPEA, DMF, 24 h. (e) 0.1 M NaOH in 4:1 MeOH/H_2O, 1 h. Ht = Hoechst 33258; g = guanidinium group.

The extent of the linker coupling reaction was determined to be 100% by UV absorbance of the released MMTr cation. The CPG was split into two portions, and one portion was coupled to **15** using PyBOP, HOBt, and DIPEA to afford the DNG−Hoechst conjugate **20** with an 11-atom linker. For the second portion, the coupling/capping/deprotection reaction cycle with **10** was repeated one more time before Hoechst acid **15** was finally coupled to afford the conjugate **21** with an 18-atom linker. The CPG beads of conjugates **20** and **21** fluoresced under long-wave UV light, indicating the successful addition of the Hoechst acid **15** onto the linker. Conjugates **20** and **21** were cleaved from CPG under very mild cleavage conditions. Direct assault with NH_4OH or methanolic ammonia solution resulted in the cleavage of conjugates from CPG, as well as the cleavage of linker between DNG and Hoechst ligand. Hence, we performed the deprotection and cleavage of DNG−Hoechst conjugates using 0.1 M NaOH solution in 4:1 methanol/water at room temperature for 1h, in which a majority of the conjugate was intact as determined by HPLC. The Fmoc protection on the guanidinium groups was also removed in the same step. After cleavage, the solution was desalted using NAP-10 columns and HPLC grade water as the solvent. The eluted solutions were turbid, possibly due to the aggregation of the conjugate. The Hoechst 33258 is known to aggregate in aqueous solutions at ∼30 μM concentrations.[25b] Addition of 0.01% TFA in water afforded a clear solution that fluoresces under long-wave UV. Purification of crude conjugates was accomplished on RP-HPLC (C_8 column) using solvent A (0.1% TFA in water) and a gradient of solvent B (acetonitrile) 5% → 80% in 30 min. Both conjugates **2** and **3** were eluted as broad peaks at ∼14 min. ESI/TOF+ analysis of conjugate **2** exhibited desired peaks at *m*/*z* 954.57 (M + 2H), 636.70 (M + 3H), and 477.79 (M + 4H); calcd 954.45 (M + 2H), 636.63 (M + 3H), and 477.72 (M + 4H) for $C_{89}H_{114}N_{30}O_{19}$. Conjugate **3** exhibited peaks at

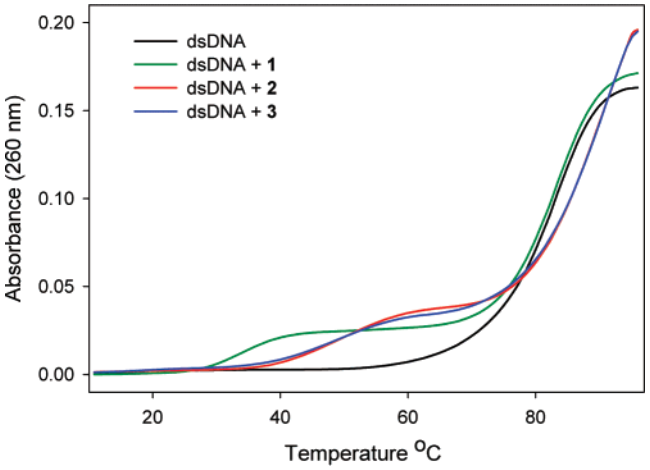

Figure 4. Normalized triplex T_m curves for 30-mer dsDNA and dsDNA + 1 equiv of **1** or **2** or **3** in 10 mM $KHPO_4$ buffer, pH 7.0, containing 100 mM KCl.

m/z 1011.04 (M + 2H), 674.35 (M + 3H), and 506.26 (M + 4H); calcd 1010.99 (M + 2H), 674.32 (M + 3H), and 505.99 (M + 4H) for $C_{95}H_{125}N_{31}O_{20}$.

Thermal Melting (T_m) Stability of $(DNA)_2$·DNG−H Triplex Complexes. The stability of triplexes formed by DNG and DNG−Hoechst conjugates was assessed by examining absorbance vs temperature plots. We chose a 30-mer DNA duplex, d(CGCCGCGCGCGCGAAAAACCCGGCGCGCGC)/d(GCGGCGCGCGCGCTTTTTGGGCCGCGCGCG), containing the pentameric AAAAA/TTTTT tract at the center as the target site. The sequence on either side of the target site is composed solely of G:C base pairs, such that the triplex formation by DNG and minor groove-binding by Hoechst ligand could occur only at the A5/T5 tract. The binding by Hoechst 33258 ligand in a dsDNA minor groove requires at least a four base pair A:T rich site.[43−45] The pentameric thymidyl DNG (**1**) forms a stable $(DNA)_2$·DNG triplex (T_m = 36 °C) at the dsDNA target site due to charge−charge interactions. Furthermore, the Hoechst 33258-tethered DNG (conjugates **2** and **3**) exhibited significant triplex stabilization compared to the DNG lacking a pendant Hoechst dye (Figure 4). Conjugates **2** and **3** formed stable $(DNA)_2$·DNG−H triplexes and exhibited a T_m of 49 °C and a ΔT_m of +13 °C compared with $(DNA)_2$·DNG triplex formed by DNG **1**, in a 10 mM potassium phosphate buffer, pH 7.0, containing 100 mM KCl (Table 1). The presence of a five base pair A:T rich site in the target dsDNA (entries 1−3, Table 1) provides effective binding site for the tethered ligand. Previous reports indicate that binding of Hoechst 33258 dye somewhat destabilizes the DNA triplex structure while stabilizing duplex.[46] However, our results show that covalent conjugation of Hoechst 33258 dye with triplex-forming DNG stabilizes both $(DNA)_2$·DNG−H triplex and target duplex due to the simultaneous binding of the DNG−Hoechst 33258 conjugate in the major and minor grooves of the target dsDNA site. These results are consistent with the results exhibited by DNA−Hoechst conjugates.[23] The change in the tether length from 18 to 11 atoms did not have any significant effect on triplex T_m (entries 2 and 3, Table 1), which indicates that the 11-atom linker is sufficient to traverse the backbone, permitting the Hoechst ligand to reside deep into the A:T rich minor groove. A significant decrease in triplex T_m values was observed with an increase in salt concentration (Table 1), which is attributed to a reduction in the electrostatic attraction between the oppositely charged backbones. Upon increasing the salt concentration from 100 mM to 700 mM KCl, while maintaining pH 7.0, the $(DNA)_2$·DNG triplex T_m was decreased by 4 °C, whereas the $(DNA)_2$·DNG−H triplex T_m was decreased by 6−7 °C. Conversely, the T_m of dsDNA was increased as expected (Figure 5). The stability of $(DNA)_2$·DNG triplex complex formed by DNG (**1**) and dsDNA is almost independent of pH. However, the stabilities of $(DNA)_2$·DNG−H triplex complexes formed by conjugates **2** and **3** with dsDNA are slightly decreased with the increase of pH (entries 2 and 3, Table 1). In $(DNA)_2$·DNG−H triplex complexes, the ligand may be binding more effectively in the dsDNA minor groove at lower pH due to the protonation of benzimidazoles[47] and interaction with the phosphodiester backbone. As anticipated from previous studies of bis-benzimidazoles,[47] the conjugates **2** and **3** exhibited significant increase in fluorescence emission with decreasing pH 8 to 6. The dependence of binding of **2** and

Table 1. Thermal Melting (T_m) and Fluorescence Emission Values of Triplexes Formed by dsDNA and DNG−Hoechst 33258 Conjugates[a]

5'-CGCCGCGCGCGCGXXXXXCCCGGCGCGCGC-3'
3'-GCGGCGCGCGCGCYYYYYGGGCCGCGCGCG-5'
Hoechst
3'-TTTTT

			T_m (°C) at pH				
entry	XXXXX YYYYY	DNG conjugate	6.0 (0.1 M)	7.0 (0.1 M)	7.0 (0.7 M)	8.0 (0.1 M)	F_{450}[b]
1	AAAAA TTTTT	**1**	38	36	32	35	−
2	AAAAA TTTTT	**2**	53	49	42	46	246
3	AAAAA TTTTT	**3**	52	49	41	46	248
4	AA**G**AA TT**C**TT	**1**	−	25	−	−	−
5	AA**G**AA TT**C**TT	**2**	−	26	−	−	34
6	AA**G**AA TT**C**TT	**3**	−	26	−	−	34
7	AA**T**AA TT**A**TT	**1**	−	26	−	−	−
8	AA**T**AA TT**A**TT	**2**	−	43	−	−	254
9	AA**T**AA TT**A**TT	**3**	−	44	−	−	262
10	A**G**A**G**A T**C**T**C**T	**1** or **2** or **3**	−	nt[c]	−	−	nf[d]

[a] T_m studies were carried out in 10 mM $KHPO_4$ buffer, pH 6.0, 7.0, or 8.0 containing 100 or 700 mM KCl as mentioned. T_m values were determined by first derivative analysis, and standard deviations are ±1 °C. The target dsDNA T_m values are 84−86 °C (pH 7.0 and 0.1M KCl); however, increased T_m (90−92 °C) values were observed in triplex state due to the binding of Hoechst moiety in the minor groove or salt concentration. [b] Values represent the fluorescence emission enhancement (in arbitrary units) at 450 nm for the 50 nM triplex complexes in 10 mM $KHPO_4$ buffer pH 7.0 containing 100 mM KCl. [c] No triplex observed.[d] No fluorescence enhancement.

(43) (a) van Dyke, M. W.; Hertzberg, R. P.; Dervan, P. B. *Proc. Natl. Acad. Sci. U.S.A.* **1982**, *79*, 5470. (b) Harshman, K. D.; Dervan, P. B. *Nucleic Acids Res.* **1985**, *13*, 4825.
(44) Portugal, J.; Waring, M. J. *Biochim. Biophys. Acta* **1988**, *949*, 158.
(45) (a) Abu-Daya, A.; Brown, P. M.; Fox, K. R. *Nucleic Acids Res.* **1995**, *23*, 3385. (b) Fox, K. R.; Waring, M. J. *Nucleic Acids Res.* **1984**, *12*, 9271.
(46) (a) Durand, M.; Thuong, N. T.; Maurizot, J. C. *Biochimie* **1994**, *76*, 181. (b) Kim, H.-K.; Kim, J.-M.; Kim, S. K.; Rodger, A.; Norden, B. *Biochemistry* **1996**, *35*, 1187.
(47) Gorner, H. *Photochem. Photobiol.* **2001**, *73*, 339.

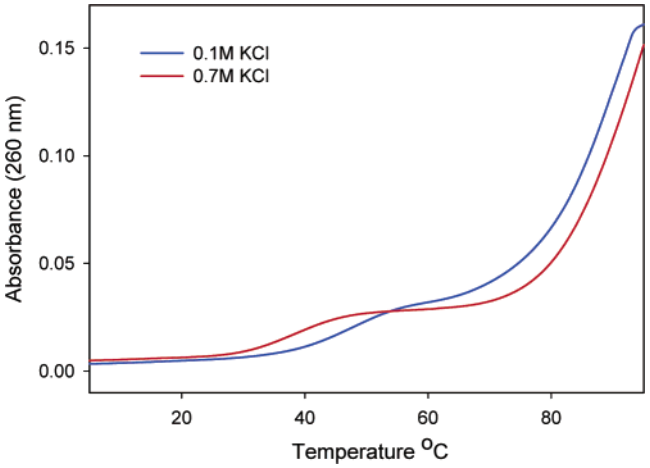

Figure 5. Normalized triplex T_m curves formed by 2 μM 30-mer dsDNA and 1 equiv of **3** in 10 mM $KHPO_4$ buffer, pH 7.0, containing 0.1 M KCl and 0.7 M KCl.

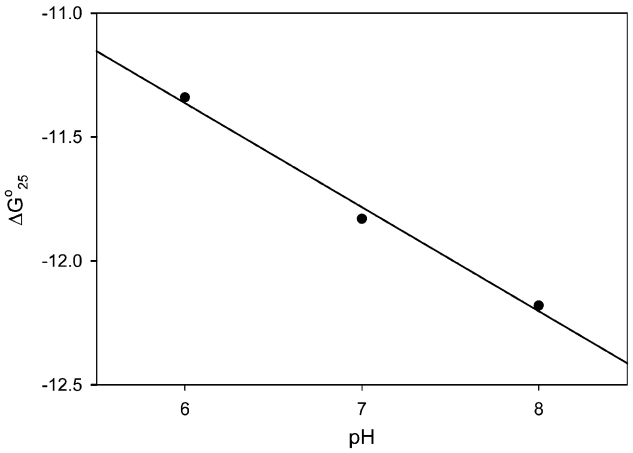

Figure 6. pH vs $\Delta G_{25}°$ (standard free energy of binding) plot. The $\Delta G_{25}°$ values for $(DNA)_2$·DNG−H formation were calculated from T_m curves.[47]

3 to dsDNA is best examined by a plot of the standard free energy of complex formation ($\Delta G_{25}°$) vs pH (Figure 6). The $\Delta G_{25}°$ values for $(DNA)_2$·DNG−H triplex formation were calculated from T_m curves.[48] Essentially, the same plot serves for both conjugates **2** and **3**. If the equilibrium constant for triplex formation required a single proton, the plot would be linear with a slope of −1. The apparently linear plot has a slope of −0.42 between pH 6 and 8. The Hoechst moiety has pK_a values at 5.5 and 8.5. Thus, the pH $-\Delta G_{25}°$ profile tends to flatten somewhat between pH 6 and 8. We may conclude that the diprotonated species binds in the minor groove better than the monoprotonated species.

To analyze the sequence selectivity in dsDNA recognition by triplex forming DNG and DNG−Hoechst conjugates, we have investigated the triplex formation between DNG conjugates (**1**−**3**) and dsDNA containing one or two mismatched base pairs in the target site. As can be seen from triplex T_m values in Table 1, a single base pair mismatch (entries 4−9) in the center of the target dsDNA site exhibited a dramatic decrease in the triplex stability. Incorporation of a G:C base pair mismatch in the center of the target dsDNA site (entries 4−6, Table 1) decreased the $(DNA)_2$·DNG triplex T_m by 11 °C (entries 1 and 4, Table 1)

(48) (a) Marky, L. A.; Breslauer, K. J. *Biopolymers* **1987**, *26*, 1601. (b) Gralla, J.; Crothers, D. M. *J. Mol. Biol.* **1973**, *78*, 301.

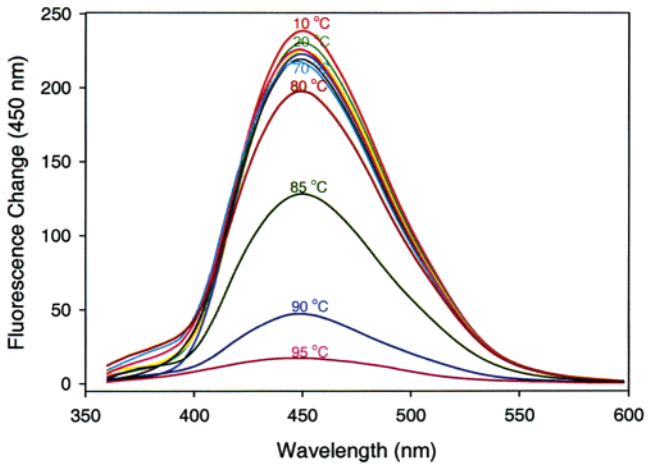

Figure 7. Change in fluorescence emission spectrum with temperature of a 50 nM solution of triplex (formed from 30-mer dsDNA and conjugate **3**) in 10 mM $KHPO_4$ buffer, pH 7.0, containing 100 mM KCl.

for DNG **1**, whereas the $(DNA)_2$·DNG−H triplex T_m values decreased by 23 °C (entries 2 and 5 or 3 and 6, Table 1) for conjugates **2** and **3**, respectively. However, inversion of an A:T base pair into a T:A base pair in the center of the binding site (entries 7−9, Table 1) decreased the $(DNA)_2$·DNG triplex T_m by 10 °C (entries 1 and 7, Table 1), whereas the $(DNA)_2$·DNG−H triplex T_m values decreased only 5−6 °C (entries 2 and 8 or 3 and 9, Table 1). It is noteworthy that both DNG (**1**) and DNG−Hoechst conjugates (**2** and **3**) exhibited essentially the same triplex T_m (25−26 °C, Table 1) values for the G:C mismatched dsDNA sequence. On the other hand, the DNG−Hoechst conjugates (**2** and **3**) exhibited enhanced triplex T_m (42−43 °C, Table 1) for the T:A mismatched dsDNA sequence. Hoechst 33258 has a stronger affinity for A:T- than G:C-containing dsDNA sequences. Incorporation of a single G:C base pair in the binding site generates a mismatch sequence for both DNG and Hoechst moieties. The inability of the tethered Hoechst ligand binding tightly in the mismatched minor groove prevents the stabilization of the triplex structure. As a result, triplexes formed by both DNG and DNG−Hoechst conjugates with G:C mismatch-containing dsDNA sequence exhibited similar T_m values (entries 4−6, Table 1). Inversion of an A:T base pair into a T:A base pair selectively generates a mismatch sequence for the DNG moiety, but serves as a favorable binding site for the Hoechst moiety. Therefore, the tethered Hoechst moiety is able to bind tightly in the A:T rich minor groove, which enhances the $(DNA)_2$·DNG−H triplex T_m by 16 to 17 °C (entries 7 and 8 or 7 and 9). With two G:C base pair mismatches (entry 10, Table 1) there is no triplex formation.

Fluorescence Characteristics of $(DNA)_2$·DNG−H Triplex Complexes. In addition to the enhanced triplex stability, as determined by T_m studies, the fluorescence emission of DNG−Hoechst conjugates was increased greatly on complexation with the target dsDNA. When excited at 345 nm, the $(DNA)_2$·DNG−H triplexes formed by conjugates **2** and **3** emit a broad fluorescent signal centered at 450 nm (Figure 7). This signal is consistent with the dsDNA/Hoechst 33258 complexes, which generally emit a broad fluorescence signal centered at 445 nm.[49−51] To confirm that the observed fluorescence signal was due to binding of tethered Hoechst 33258 fluorophore in the minor groove of target dsDNA, we examined the temperature effects of the fluorescence emission spectra. The fluorescence

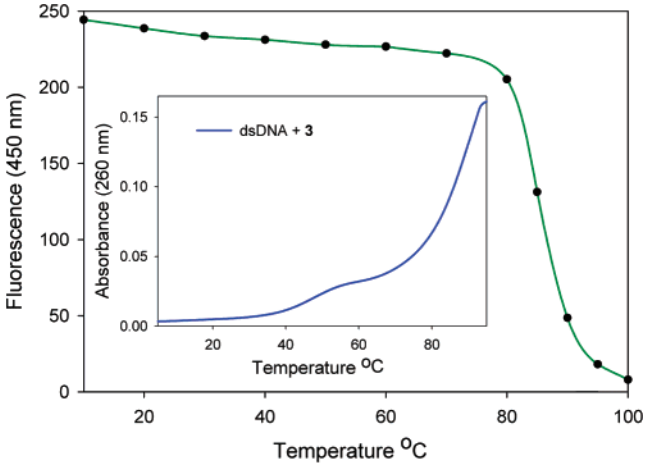

Figure 8. Fluorescence change vs temperature plot of a 50 nM triplex (formed by conjugate **3** and 30-mer dsDNA) in 10 mM $KHPO_4$ buffer, pH 7.0, containing 100 mM KCl. Inset: absorbance vs temperature plot for the same triplex.

signal decreases with increase in temperature, and the change becomes dramatic in the DNA duplex T_m (~84 °C) range (Figure 7). An examination of fluorescence vs temperature plot (Figure 8) for this $(DNA)_2$·DNG−H triplex complex reveals that there is only a marginal decrease in the fluorescence emission until ~70 °C, that is even after the DNG third strand was separated from the major groove (triplex T_m = 49 °C). However, the fluorescence emission dropped tremendously upon reaching the duplex DNA T_m (~84 °C) range, which indicates that the Hoechst fluorophore is binding solely in the Watson−Crick minor groove of the target dsDNA and not anywhere else in the $(DNA)_2$·DNG−H triplex region.

The fluorescence emission of the DNG−Hoechst conjugates increased by 246−248 (arbitrary) units upon hybridization with the dsDNA containing the five A:T base pair binding site (entries 2 and 3, Table 1). Introduction of a G:C base pair mismatch in the center of the target dsDNA sequence (entries 4−6, Table 1) exhibited fluorescence emission enhancement to only 34 units due to the inhibition of Hoechst fluorophore's binding. No fluorescence emission enhancement was observed in the presence of two G:C base pair mismatches in the binding site (entry 10, Table 1). This indicates that Hoechst fluorophore of conjugates **2** and **3** is not binding in the G:C mismatch-containing minor groove site and is therefore unable to enhance the $(DNA)_2$·DNG triplex stability as observed in the triplex T_m study (entries 4−6 and 10, Table 1). However, the triplex complexes formed by T:A mismatch-containing sequence exhibited fluorescence emission enhancement to 254−262 units (entries 8 and 9, Table 1) similar to that of triplex complexes formed by nonmismatch sequence (entries 2 and 3, Table 1). Furthermore, the temperature vs fluorescence behavior of these triplex complexes is consistent with the triplex complexes formed by nonmismatch dsDNA sequence. These observations support the assertion (Figure 3) that complexation of DNG−Hoechst 33258 conjugates with dsDNA target site results in the formation of a local $(DNA)_2$·DNG−H triplex in which the DNG strand occupies the major groove and Hoechst ligand binds in the Watson−Crick minor groove simultaneously.

Table 2. Thermal Melting (T_m) and Fluorescence Emission Values of Duplexes Formed by DNA and DNG−Hoechst Conjugates[a]

entry	DNA	DNG conjugate	T_m (°C)	F_{475}[d]
1	AAAAA	**1**	43	−
2	AAAAA	**2**	45	24
3	AAAAA	**3**	45	26
4	AA**C**AA	**1**	35	−
5	AA**C**AA	**2**	36	nf[e]
6	AA**C**AA	**3**	36	nf[e]
7	**C**AAAA	**1**	38	−
8	**C**AAAA	**2**	39	nf[e]
9	**C**AAAA	**3**	39	nf[e]
10	AAAA**C**	**1**	36	−
11	AAAA**C**	**2**	38	nf[e]
12	AAAA**C**	**3**	38	nf[e]
13	30-mer[b]	**2**	50[c]	278
14	30-mer[b]	**3**	50[c]	272

[a] T_m studies were carried out at 6 μM concentrations in 10 mM $KHPO_4$ buffer, pH 7.0, containing 100 mM KCl. T_m values were determined by first derivative analysis, and standard deviations are ±1 °C. The DNA oligomers are all pentamers unless stated otherwise. [b] 30-mer ssDNA sequence is 5′-CGCCGCGCGCGCGAAAAACCCGGCGC GCGC-3′. [c] T_m determined from fluorescence vs temperature plot. [d] Values represent the fluorescence emission enhancement (in arbitrary units) at 475 nm for the 560 nM duplex complexes in 10 mM $KHPO_4$ buffer, pH 7.0, containing 100 mM KCl. [e] No fluorescence enhancement observed.

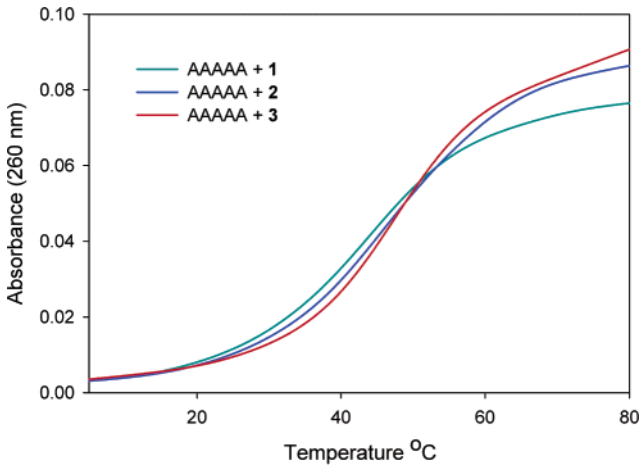

Figure 9. Normalized duplex T_m curves formed by ssDNA and 1 equiv of **1** or **2** or **3** in 10 mM $KHPO_4$ buffer, pH 7.0, containing 100 mM KCl.

Thermal Melting (T_m) Stability of DNA·DNG−H Duplex Complexes. The DNA·DNG duplex is stabilized by electrostatic attractions.[19] The generated minor groove of DNA·DNG duplex is slightly different[35] from that of the minor groove of dsDNA, and the binding properties of Hoechst ligand are unknown. To determine the effect of tethered Hoechst ligand on the stability of DNA·DNG duplex by binding in the generated minor groove, we have examined thermal melting characteristics when the DNG is lacking or tethering a pendant Hoechst ligand. The duplex formation and stability was monitored by temperature vs absorbance at 260 nm. The complementary and mismatch DNA sequences chosen for this study and the observed T_m values are summarized in Table 2.

The DNA·DNG duplex formed by pentameric thymidyl DNG (**1**) and complementary pentameric adenyl DNA exhibited a T_m of 43 °C, whereas the DNA·DNG−H duplexes formed from pentameric adenyl DNA and DNG−Hoechst conjugate (**2** or **3**) exhibited a T_m value of 45 °C (ΔT_m = +2 °C) (Figure 9).

(49) (a) Loontiens, F. G.; Regenfuss, P.; Zechel, A.; Dumortier, L.; Clegg, R. M. *Biochemistry* **1990**, *29*, 9029. (b) Loontiens, F. G.; McLaughlin, L. W.; Diekmann, S.; Clegg, R. M. *Biochemistry* **1991**, *30*, 182.
(50) Haq, I.; Ladbury, J. E.; Chowdhry, B. Z.; Jenkins, T. C.; Chaires, J. B. *J. Mol. Biol.* **1997**, *271*, 244.
(51) Bostock-Smith, C. E.; Searle, M. S. *Nucleic Acids Res.* **1999**, *27*, 1619.

```
5'                  CGCCGCGCGCGCGAAAAACCCGGCGCGCGC
                    ||||||||||
3' CGCGCGCGGCCCAAAAAGCGCGCGCGCCGC

5' CGCCGCGCGCGCGAAAAACCCGGCGCGCGC
                           ||||||||
3'                         CGCGCGCGGCCCAAAAAGCGCGCGCGCCGC

5'                    CGCCGCGCGCGCGAAAAACCCGGCGCGCGC
                      ||||||||
3' CGCGCGCGGCCCAAAAAGCGCGCGCGCCGC

5' CGCCGCGCGCGCGAAAAACCCGGCGCGCGC
       ||||||||           ||||||||
3'     CGCGCGCGGCCCAAAAAGCGCGCGCGCCGC
```

Figure 10. Possible self-dimers of 30-mer ssDNA sequence 5′-CGCCGCGCGCGAAAAACCCGGCGCGCGC-3′.

This marginal increase, when compared with that of 30-mer $(DNA)_2$·DNG−H triplex (ΔT_m of +13 °C, Table 1), indicates very weak binding by Hoechst ligand in the minor groove of pentameric DNA·DNG duplex. Our molecular dynamics studies of a DNA·DNG duplex revealed that the charge−charge attractions between oppositely charged backbones reduce the width of the DNA·DNG minor groove by 0.7 Å.[35] Under the experimental conditions, the piperazine ring of the Hoechst dye carries a positive charge,[23] as does the guanidinium group. The narrower minor groove of DNA·DNG duplex and charge−charge repulsion effects may not allow the Hoechst dye, possessing a bulky and nonplanar *N*-methylpiperazine ring, to penetrate deep into the floor of the minor groove for effective binding.

As we have seen, complexation of DNG−Hoechst conjugates **2** or **3** with the 30-mer ssDNA sequence, 5′-CGCCGCGCGCGC-GAAAAACCCGGCGCGCGC-3′, is accompanied by considerable enhancement in the observed fluorescence emission (see fluorescence characteristics). The presence of a long sequence of G:C base pairs on either side of the target adenyl site provides a flexible DNA·DNG minor groove in which the tethered Hoechst fluorophore can fit. As a result, the fluorescence emission was enhanced by 278 units. However, this 30-mer sequence did not aid in determining the DNA·DNG−H duplex T_m value because of the long self-dimers (Figure 10), formed by G:C sequences of the ssDNA, and whose T_m profile was more dominate. However, the analysis of fluorescence vs temperature plot (see duplex fluorescence) revealed the DNA·DNG−H duplex $T_m \approx 50$ °C ($\Delta T_m = \sim 7$ °C; see entries 1 and 14, Table 2).

To analyze the sequence specificity, we have investigated the duplexes between DNG conjugates (**1**−**3**) and complementary DNA containing one mismatched base either at the end of the sequence or in the center (Table 2). Incorporation of a single cytidine mismatch in the complementary DNA sequence exhibited significant decrease in DNA·DNG duplex T_m values (Table 2), and an internal mismatch exhibited a much more pronounced effect ($\Delta T_m = -8$ °C, entries 1 and 4) than a terminal mismatch[19c] ($\Delta T_m = -5$ °C, entries 1 and 7). The duplexes formed by DNG conjugates **1**−**3** with complementary DNA sequences were independent of pH over the range 6.0−8.0. The tethered Hoechst derivative did not exhibit any significant effect on the DNA·DNG duplex stability at either lower or higher pH because of its poor binding.

Fluorescence Characteristics of DNA·DNG−H Duplex Complexes. Upon complexation of conjugates **2** and **3** with complementary pentameric ssDNA, a DNA·DNG−H duplex will be formed and the fluorescence signal of the Hoechst dye should increase if it can fold back and bind in the generated minor groove. When excited at 345 nm, the DNA/DNG−Hoechst conjugate (**2** or **3**) complexes (entries 2 and 3, Table 2) emitted a weak (24-unit increase) fluorescence signal centered at 475 nm, suggesting the Hoechst fluorophore's inability to bind effectively in the minor groove of pentameric DNA·DNG. However, upon complexation with 30-mer ssDNA sequence, 5′-CGCCGCGCGCGCGAAAAACCCGGCGCGCGC-3′, the fluorescence emission of conjugates **2** and **3** was increased greatly, by 278 units at 475 nm (see Supporting Information). This signal is red-shifted by 25 nm with respect to the triplex fluorescence signal, which emits a broad signal centered at 450 nm (Figure 7). However, the intensity of the emission signal was ∼10-fold less than that of the triplex fluorescence emission signal at the same concentrations. This weak binding of fluorophore may be attributed to charge−charge repulsions between protonated piperazine ring and guanidinium groups and/or differences in the shape of the minor groove.

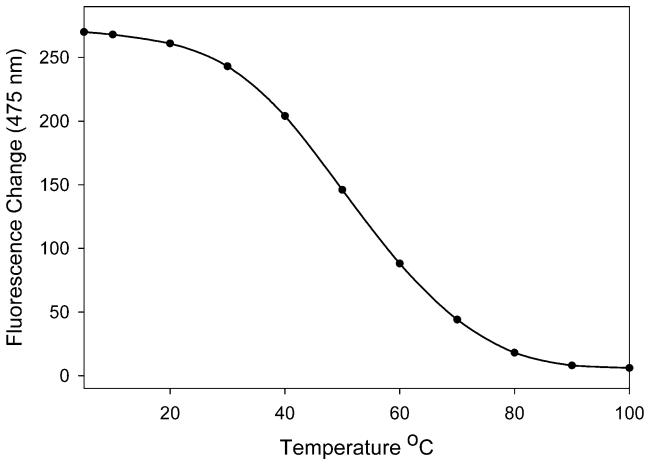

Figure 11. Fluorescence change vs temperature plot for duplex formed by conjugate **3** and 30-mer ssDNA sequence, 5′-CGCCGCGCGCGC-GAAAAACCCGGCGCGCGC-3′) in 10 mM $KHPO_4$ buffer, pH 7.0, containing 100 mM KCl.

To confirm that the observed fluorescence emission was a result of binding of the Hoechst 33258 fluorophore in the DNA·DNG minor groove, we studied the temperature vs fluorescence emission characteristics of DNA·DNG−H duplex formed by 30-mer ssDNA and conjugate **3**. A plot of fluorescence vs temperature revealed that the relationship is sigmoidal (Figure 11). Analysis of Figure 11 shows a midpoint in fluorescence emission occurring at ∼50 °C, which is higher by ∼5−7 °C than the T_m values (43−45 °C, entries 1−3, Table 2) of duplexes formed by pentameric DNA and DNG−Hoechst conjugates. These results support that the Hoechst ligand is able to bind in the DNA·DNG minor groove and provides enhanced duplex stability.

Conclusions

Positively charged thymidyl DNG, an analogue of DNA, was synthesized on solid phase in a 3′ → 5′ direction, and Hoechst 33258 ligand was tethered via 11 and 18 atom linkers to the 5′-terminus of DNG using PyBOP/HOBt chemistry. We have shown that hybridization of DNG−Hoechst conjugates to the target dsDNA enhances the $(DNA)_2$·DNG−H triplex stability through simultaneous minor groove binding by tethered Hoechst

33258 fluorophore. Furthermore, when provided with a flexible minor groove, the Hoechst fluorophore is able to bind in the DNA·DNG minor groove and further enhances the duplex stability and fluorescence emission significantly. The nuclease resistant guanidine linkages and the tethered Hoechst fluorophore are expected to enhance the cellular and nuclear membrane permeability of these DNG conjugates. Investigation of the cell invasion and possible antisense/antigene characteristics of these conjugates is in progress.

Experimental Section

Materials. Unless otherwise noted, all solvents and reagents were obtained from Aldrich and used without further purification. TLCs were carried out on commercially available flexible TLC silica gel (Silica gel 60 F_{254}) plates purchased from Selecto Scientific, and compounds on TLC were visualized using shortwave UV light. Silica gel (pore size: 32−63 Å, Selecto Scientific) was used for flash column chromatography. All NMR spectra were recorded on a Varian 400 MHz instrument. HRMS (ESI/TOF+) mass spectral analysis was performed on a Micromass Q-Tof-2 quadrapole instrument. Long chain alkylamine CPG (pore size: 500 Å; mesh size: 80−120) was obtained from Sigma and soaked in and washed with dry DMF before use. DNA oligomers were purchased as prepurified from the Biomedical Resource Center at UCSF.

NAP-10 (Sephadex G25 DNA grade) columns were purchased from Amersham Biosciences. HPLC grade acetonitrile and water were purchased from Fisher Scientific, and triethylammonium acetate (TEAA) buffer was purchased from Aldrich. Reverse-phase HPLC was performed on a Hewlett Packard 1050 instrument equipped with a quaternary solvent delivery system and a diode array detector. Alltech Macrosphere 300 Å, C8, silica 7 μm, 250 mm × 10 mm preparative reverse-phase column was used. UV detector was set at 260 nm for DNG or 260 and 343 nm for DNG−Ht. A gradient from 90% → 20% eluent A (0.1% TFA in water) and 10% → 80% eluent B (acetonitrile) over 30 min with a flow rate of 3.0 mL/min was used.

DNA, DNG, and DNG−Ht Conjugates Extinction Coefficients. The DNA and DNG (**1**) extinction coefficients at 260 nm were determined according to the nearest neighbor method, and for the conjugates (**2** and **3**) the extinction coefficient of the Hoechst acid (**15**) at 260 nm (20800 A_{260} units mM^{-1}) was added to the calculated value of DNG. However, the concentrations of conjugates solutions were determined using the extinction coefficient (46400 A_{347} units M^{-1}) of Hoechst acid **15**.

Thermal Melting (T_m) Studies. All T_m experiments were carried out in 10 mM potassium phosphate buffer, pH 6.0, 7.0, or 8.0 containing 100 or 700 mM KCl, as mentioned, at oligomer concentrations of 2 μM (for triplex) and 6 μM (for duplex). The solutions were annealed by heating to 95 °C using a heating block and allowing to cool slowly to reach room temperature before being stored at 4 °C. Absorbance (260 nm) vs temperature values were obtained on a Cary 100 Bio UV/vis spectrophotometer equipped with a temperature programmable cellblock. Data points between 5 and 95 °C were taken for every 1 °C, with a temperature ramp of 0.5 °C/min. T_m temperatures were calculated by first-derivative analysis and also by direct graphical analysis of the absorbance vs temperature plot to determine the midpoint of the transition. Both techniques gave values that were within the experimental error (±1 °C) for the analysis. Also, we have carried out a concentration-dependent T_m study to rule out the possibility of intramolecular duplex formation.

Fluorescence Emission Studies. Fluorescence spectra were obtained on a Perkin-Elmer LS50B fluorophotometer equipped with a constant-temperature water bath set at 25 °C. All measurements were performed with the following parameters: slit width, Ex/Em = 10 nm/10 nm; high sensitivity; high speed 500 nm/s. Solutions in 10 mM potassium phosphate buffer pH 7.0 containing 100 mM KCl were introduced into a 2.5 mL quartz cell thermally isolated with a water jacket. Solutions at concentrations of 50 nM were excited at 345 nm, and emissions were monitored between 360 and 600 nm. Temperature vs fluorescence spectra were obtained by controlling the temperature with a recirculating water bath. Emission spectra were recorded with λ_{ex} = 345 nm.

Synthesis: 9-(3,5-Di-*O*-mesyl-2,3,5-trideoxy-*β*-D-*threo*-pentofuranosyl)thymidine (6). Mesyl chloride (1.55 mL, 20 mmol) was added dropwise via syringe to an ice-cold solution of **5**[36] (0.97 g, 4 mmol) in dry pyridine (20 mL) under argon atmosphere. The reaction mixture was allowed to reach room temperature over ∼4 h and was then stirred overnight. The pyridine was rotoevaporated, and the residue was partitioned between chloroform and water. Aqueous layer was extracted with 3 × 100 mL of chloroform. The combined chloroform layer was dried, treated with charcoal, and rotoevaporated. The product was pure and was used for further reactions without purification, yield 1.52 g, (96%). ^{1}H NMR (DMSO-d_6, 400 MHz): δ 1.79 (s, 3H, −CH_3), 2.31 (m, 1H, 2′-H), 2.87 (m, 1H, 2″-H), 3.26 (s, 3H, mesyl CH_3), 3.32 (s, 3H, mesyl CH_3), 4.37 (m, 1H, 3′-H), 4.48 (m, 1H, 5′H), 4.55 (m, 1H, 5″-H), 5.38 (m, 1H, 4′-H), 6.20 (m, 1H, 1′-H), 7.45 (s, 1H, −CH−), 11.39 (s, 1H, −NH−). ^{13}C NMR (DMSO-d_6, 400 MHz): 12.34, 36.85, 37.68, 38.08, 67.79, 78.66, 79.11, 83.08, 109.88, 135.43, 150.46, 163.68. HRMS (ESI/TOF+) *m*/*z*: 399.0528 (M + H); calcd 399.0532 (M + H) for $C_{12}H_{18}N_2O_9S_2$.

3,5-Diamino-2,3,5-trideoxythymidine (7). Lithium azide (3.43 g, 70 mmol) was suspended in a solution of **6** (1.39 g, 3.5 mmol) in dry DMF (35 mL) and stirred at 100 °C for 4 h. The reaction mixture was cooled to room temperature, and DMF was rotoevaporated under vacuum. Residue was partitioned between chloroform and water. Aqueous layer was extracted with 3 × 100 mL chloroform. The combined chloroform layer was dried and rotoevaporated. The residue was purified on silica gel column using 0−5% methanol in dichloromethane to yield 0.74 g (73%) of pure 3,5-diazido-2,3,5-trideoxythymidine. ^{1}H NMR (DMSO-d_6, 400 MHz): δ 1.76 (s, 3H, −CH_3), 2.47 (m, 1H, 2′-H), 2.59 (m, 1H, 2″-H), 3.47 (m, 1H, 5′-H), 3.58 (m, 1H, 5″-H), 4.37 (m, 1H, 3′-H), 5.27 (m, 1H, 4′-H), 5.88 (t, *J* 4, 1H, 1′-H), 7.60 (s, 1H, −CH−). HRMS (ESI/TOF+) *m*/*z*: 293.1093 (M + H); calcd 293.1111 (M + H) for $C_{10}H_{12}N_8O_3$. To a solution of 3,5-diazido-2,3,5-trideoxythymidine (0.65 g, 2.25 mmol) in 95% ethanol (50 mL) was added 50 mg of 10% Pd/C and hydrogenated at 50 psi for 4 h. The solution was filtered through Celite, and the filtrate was rotoevaporated to dryness under reduced pressure. The residue was further dried overnight under high vacuum to give a quantitative yield of the pure compound **7**. ^{1}H NMR (DMSO-d_6, 400 MHz): δ 1.79 (s, 3H, −CH_3), 2.01 (m, 1H, 2′-H), 2.13 (m, 1H, 2″-H), 2.82 (m, 1H, 5′-H), 2.89 (m, 1H, 5″-H), 3.37 (m, 1H, 4′-H), 3.48 (m, 1H, 3′-H), 6.10 (t, *J* = 7 Hz, 1H, 1′-H), 7.64 (s, 1H, −CH−). ^{13}C NMR (DMSO-d_6, 400 MHz): 12.16, 39.84, 42.61, 52.13, 83.14, 86.52, 109.53, 136.53, 150.46, 163.80. HRMS (ESI/TOF+) *m*/*z*: 241.1293 (M + H); calcd 241.1301 (M + H) for $C_{10}H_{16}N_4O_3$.

5′-Monomethoxytritylamino-3′-(*N*′-9-fluorenylmethoxycarbonylthiouria)-2′,3′,5′-trideoxythymidine (8). Monomethoxytrityl chloride (1.73 g, 5.6 mmol) in dry dichloromethane (10 mL) was added dropwise to a solution of **7** (1.35 g, 5.6 mmol) and triethylamine (1.56 mL, 11.2 mmol) in dry DCM (100 mL) at 0 °C. After being stirred at room temperature for 4 h, TLC showed the completion of the reaction. Reaction mixture was diluted with another 100 mL of DCM and washed with water (2 × 100 mL). The DCM layer was dried and rotoevaporated to solid. The crude product was purified on a silica gel column using 0−1% methanol in DCM containing 0.5% TEA to yield 2.26 g (91%) of pure 5′-momomethoxytritylamino-3′-amino-2′,3′,5′-trideoxythymidine. ^{1}H NMR (DMSO-d_6, 400 MHz): δ 1.70 (s, 3H, −CH_3), 2.01 (m, 1H, 2′-H), 2.14 (m, 1H, 5′-H), 2.20 (m, 1H, 5″-H), 2.35 (m, 1H, 2″-H), 2.63 (m, 1H, 3′-H), 3.60 (m, 1H, 4′-H), 3.72 (s, 3H, −OCH_3), 6.08 (t, *J* = 6 Hz, 1H, 1′-H), 6.84 (d, *J* = 9 Hz, 2H, Ar−H), 7.18 (t, 2H, *J* = 7 Hz, Ar−H), 7.29 (m, 6H, Ar−H and −CH−), 7.40 (m, 5H, Ar−H). ^{13}C NMR (DMSO-d_6, 400 MHz): 12.21, 40.31, 45.72, 52.74,

54.98, 69.77, 83.19, 85.89, 109.40, 113.07, 126.09, 127.75, 128.31, 129.65, 136.01, 137.82, 146.31, 150.42, 157.41, 163.76, 178.96. HRMS (ESI/TOF+) *m/z*: 513.2483 (M + H); calcd 513.2502 (M + H) for $C_{30}H_{32}N_4O_4$. The above product (1.53 g, 3 mmol) was dissolved in dry DCM (30 mL), and 9-fluorenylmethoxycarbonyl isothiocyanate[39] (Fmoc-NCS) (0.87 g, 3.1 mmol) was added portion wise at room temperature. After the solution was stirred for 2 h at room temperature, TLC (20:1 DCM/methanol) indicated the completion of the reaction. The solvent was rotoevaporated, and the residue was redissolved in 5 mL of DCM containing 10% methanol and precipitated by adding excess hexanes with vigorous stirring. The precipitate was filtered and dried to get pure product **8** as white solid, yield 2.1 g (89%). ^{1}H NMR (DMSO-d_6, 400 mHz): δ 1.74 (s, 3H, T-CH_3), 2.26 (m, 1H, 2′-H), 2.37 (m, 2H, 5′ and 5″-H), 2.53 (m, 1H, 2″-H), 2.87 (m, 1H, 4′-H), 3.69 (s, 3H, $-OCH_3$), 4.02 (m, 1H, 4′-H), 4.22−4.44 (m, 4H, Fmoc $-CH-$ and $-CH_2-$), 5.12 (m, 1H, 3′-NH−), 6.16 (t, J = 6 Hz, 1H, 1′-H), 6.81 (d, J = 9 Hz, 2H, Ar−H), 7.15 (t, 2H, J = 7 Hz, Ar−H), 7.22−7.45 (m, 6H, Ar−H), 7.65 (s, 1H, T-CH), 7.81−7.92 (m, 5H, Ar−H), 10.03 (d, J = 7, 1H, −NH−Fmoc), 11.35 (s, 1H, 5′-NH), 11.55 (s, 1H, T-NH). ^{13}C NMR (DMSO-d_6, 400 MHz): 12.51, 39.84, 46.01, 54.92, 67.35, 69.69, 81.98, 83.20, 109.68, 113.06, 120.09, 121.37, 125.55, 126.05, 127.21, 127.68, 127.81, 128.25, 128.91, 129.59, 136.34, 137.41, 137.66, 139.40, 140.71, 142.56, 143.27, 146.18, 150.33, 150.41, 153.25, 157.37, 163.72, 179.56. HRMS (ESI/TOF+) *m/z*: 794.2996 (M + H); calcd 794.3012 (M + H) for $C_{46}H_{43}N_5O_6S$.

6-Monomethoxytritylamino-hexanoic Acid (10). Monomethoxytrityl chloride (3.71 g, 12 mmol) in dry pyridine (25 mL) was added dropwise to a solution of **9** (1.31 g, 10.0 mmol) in dry pyridine (50 mL) at room temperature. After addition, the reaction mixture was stirred at room temperature overnight. Pyridine was rotoevaporated to dryness, and the residue was partitioned between ether and water. The aqueous layer was extracted with ether twice more (2 × 100 mL), and the combined ether layer was dried and rotoevaporated. The residue was purified by silica gel column chromatography using 0−2% methanol in DCM, yield 3.2 g (79%). ^{1}H NMR (DMSO-d_6, 400 mHz): δ 1.26 (m, 2H, $-CH_2-$), 1.43 (m, 4H, 2× $-CH_2-$), 1.94 (t, J = 7, 2H, $-CH_2COOH$), 2.16 (t, J = 7, 2H, $-NH-CH_2-$), 3.71 (s, 3H, $-OCH_3$), 6.84 (dd, J = 9, 3, 2H, Ar−*H*), 7.16 (t, J = 7, 2H, Ar−*H*), 7.27 (m, 6H, Ar−*H*), 7.38 (dd, J = 8, 2, 4H, Ar−*H*). ^{13}C NMR (DMSO-d_6, 400 MHz): 25.19, 27.17, 30.47, 34.30, 43.90, 55.60, 70.51, 113.61, 126.53, 128.28, 128.95, 130.21, 138.85, 147.28, 157.94, 175.19. HRMS (ESI/TOF+) *m/z*: 404.2201 (M + H) and 426.2037 (M + Na); calcd 404.2225 (M + H) and 426.2045 (M + Na) for $C_{26}H_{29}NO_3$.

Benzyl 4-(4-Formylphenoxy)butanoate (12). To a solution of 4-hydroxybenzaldehyde (3.3 g, 27 mmol) and benzyl 4-bromobutyrate[41] (**11**, 7.71 g, 30 mmol) in dry DMA (50 mL) was added Cs_2CO_3 (10.74 g, 33 mmol), and the solution was stirred at 100 °C for 15 h. The reaction mixture was then cooled to room temperature, and the solid was filtered off. DMA was rotoevaporated completely under high vacuum, residue was dissolved in dry DCM (250 mL), and insoluble material was filtered off. The DCM solution was then washed with water (100 mL), 2N NaOH solution (2 × 100 mL), and brine (100 mL). The DCM layer was dried with Na_2SO_4, treated with activated charcoal, and rotoevaporated. The residue was further dried under high vacuum overnight to afford pure compound **12**, yield 7.9 g (98%). ^{1}H NMR ($CDCl_3$, 400 MHz): δ 1.17 (m, 2H, $-CH_2-$), 2.60 (t, 2H, J = 7, $-CH_2-$), 4.09 (t, 2H, J = 6, $-CH_2-$), 5.14 (s, 2H, $-CH_2-$), 6.96 (dd, 2H, J = 9, 2, Ar−H), 7.35 (m, 5H, Ar−H), 7.82 (dd, 2H, J = 9, 2, Ar−H). ^{13}C NMR (400 MHz, $CDCl_3$): δ 24.58, 30.80, 66.62, 67.20, 114.91, 128.46, 128.52, 128.80, 130.14, 132.20, 135.99, 164.01, 173.01, 191.04. HRMS (ESI/TOF+) *m/z*: 299.1274 (M + H); calcd 299.1283 (M + H) for $C_{18}H_{18}O_4$.

Synthesis of Benzyl Ester of Hoechst Acid (14). A mixture of aldehyde **12** (596 mg, 2 mmol) and diamine **13**[42] (640 mg, 2 mmol) in nitrobenzene (20 mL) was stirred at 130 °C for 24 h. The solution was cooled to room temperature, and an excess of hexanes was added to precipitate the product. The precipitated crude product was collected by filtration and then purified by silica gel flash column chromatography using 9:1 ethyl acetate/methanol containing 0.1% triethylamine. Yield 1.04 g (87%), R_f = 0.2 (silica, 7:3 ethyl acetate/methanol containing 0.1% of triethylamine mixture). ^{1}H NMR (400 MHz, DMSO-d_6): δ 2.05 (m, 2H, $-CH_2-$), 2.28 (s, 3H, CH_3-NR_2), 2.51−2.59 (m, 6H, piperazine $-CH_2-$ and $-CH_2C(O)-$), (3.14 (s, 4H, piperazine $-CH_2-$), 4.10 (t, J = 6, 2H), 5.13 (s, 2H, Ar$-CH_2-$), signals detected between 6.9 and 8.4 ppm are due to Ar protons, 6.93 (m, 2H), 7.11 (d, J = 7, 2H), 7.37 (m, 5H), 7.60 (m, 2H), 8.00 (m, 1H), 8.14 (dd, 2H, J = 9, 3), 8.35 (s, 1H); HRMS (ESI/TOF+) *m/z*: 601.2911 (M + H); calcd 601.2927 (M + H) for $C_{36}H_{36}N_6O_3$.

Synthesis of Ht Acid (15). Compound **14** (1.02 g, 1.7 mmol) was dissolved in ethanol (100 mL), and 250 mg of 10% Pd/C was added and hydrogenated on a hydrogenator for 5 h under 50 psi. The solution was filtered and retoevaporated under reduced pressure. The residue was redissolved in DCM containing 10% methanol, rotoevaporated, and dried under high vacuum overnight. The product **15** was pure, and the yield was quantitative. ^{1}H NMR (DMSO-d_6, 400 MHz): δ 1.98 (m, 2H, $-CH_2-$), 2.26 (s, 3H, CH_3-NR_2), 2.42 (t, J = 7, 2H, $-OCH_2-$), 2.52 (bs, 4H, piperazine $-CH_2-$), 3.13 (bs, 4H, piperazine $-CH_2-$), 4.07 (t, J = 6, 2H, $-CH_2-COOH$), signals detected between 6.9 and 8.4 ppm are due to Ar protons, 6.92 (m, 1H), 7.13 (d, J = 9, 2H), 7.46 (m, 1H), 7.65 (m, 1H), 8.00 (m, 1H), 8.15 (d, 2H, J = 9), 8.28 (m, 1H). HRMS (ESI/TOF+) *m/z*: 511.2439 (M + H) and 533.2267 (M + Na); calcd 511.2457 (M + H) and 533.2277 (M + Na) for $C_{29}H_{30}N_6O_3$.

Solid-Phase Synthesis of DNG 1. The solid-phase synthesis of **1** was accomplished using long chain alkylamine controlled pore glass (CPG). The 5′- modified monomer[19a] was loaded on to the CPG as its succinyl derivative **4** by adopting the literature procedure[52] (see Supporting Information). The unloaded amine sites on CPG were terminated by capping with acetic anhydride/TEA, and then 5′-MMTr was deprotected with 3% DCA in DCM solution. The loading yield, 39.6 μmol/g, was determined spectrophotometrically from the amount of MMTr cation released. Synthesis of pentameric thymidyl DNG **1** was started on 15 μmol scale to accomplish conjugates **2** and **3** also on a 5 μmol scale each. A solution of **8** (59 mg, 75 μmol, 5 equiv) in 1 mL of DMF was poured over the beads. Then 1 mL of a 200 mM $HgCl_2$ solution and 1 mL of a 250 mM TEA solution in DMF were added quickly and simultaneously via two syringes. A thick white precipitate was formed immediately. The tube was capped tightly and agitated at room temperature for 2 h. The solution was filtered off, and beads were washed with DMF until all the visible precipitate has been removed. However, the CPG beads were darkened due to the black precipitate (HgS) formed in the reaction. A solution of 20% thiophenol in DMF (5 mL) was poured over the beads and agitated for 1 min to remove any black HgS precipitate. Finally, beads were washed with copious amounts of DMF followed by 1% TEA in DMF, and the coupling reaction was repeated two more times to increase the coupling yield of **16**. After the third coupling (**16**), the whole cycle of capping/deprotection/coupling was repeated three more times to get the desired pentameric DNG **17**, which was then deprotected/cleaved from CPG. Before cleaving the DNG oligomer from the CPG, one-third of the beads (~5 μmol) were separated from the SPS tube, washed with methanol, followed by DCM, and dried under vacuum. The dried beads were then transferred into a vial, and methanolic ammonia (5 mL) was poured over the beads. The vial was capped tightly and agitated at room temperature for 2 h. The supernatant solution was filtered and lyophilized to get white residue of 5′-MMTr protected DNG oligomer. The crude trityl-on product was purified on reverse-phase HPLC using 5 → 80% gradient of acetonitrile in 100 mM TEAA buffer, pH 7.0,

(52) Atkinson, T.; Smith, M. Solid-Phase Synthesis of Oligodeoxyribonucleotides by the Phosphite-Triester Methods. In *Oligonucleotide Synthesis: A Practical Approach*; Gain, M. J., Ed.; Oxford University Press: New York, 1990; pp 35−48.

and characterized by ESI mass spectrometry. To the trityl-on DNG was added 3% DCA in DCM (1 mL) and agitated for 1 min. Excess of hexanes was added to precipitate the trityl-off DNG **1**. The solvents were decanted after centrifugation, and the product was dried and analyzed by RP-HPLC.

Solid-Phase Synthesis of DNG−Hoechst 33258 Conjugates (2 and 3). After making pentameric DNG **17**, the unreacted 5′-NH_2 sites of 2/3 CPG (∼10 μmol) were capped with acetic anhydride/TEA. The linker **10** and Hoechst acid **15** were added stepwise on to **17** in the presence of PyBOP/HOBt. Both Hoechst-tethered DNGs, **2** and **3**, were synthesized on 5 μmol scale each as described below (Scheme 6).

(a) Capping. Acetic anhydride (1 mL, 200 mM) and TEA (1 mL, 250 mM) solutions in DMF were added to CPG beads (**17**), and the mixture was agitated for 10 min. The solutions were filtered off, and the beads were washed thoroughly with DMF and DCM, followed by DMF.

(b) Deprotection. The 5′-MMTr groups of **17** were cleaved by treatment with DCA solution. A solution of 3% DCA in DCM (3 mL) was poured over the beads, and the mixture was agitated for 1 min. The solution was filtered, and beads were washed with 3% DCA solution until no more yellow color was present in the filtrate. The combined filtrate was made up to a known volume, and yield was determined from UV absorbance. Before proceeding to the next coupling reaction, the CPG beads were washed thoroughly with DMF, DCM, and DMF, followed by 1% TEA in DMF solution.

(c) Coupling of Linker 10. Compound **10** (40 mg, 0.1 mmol, 10 equiv), PyBOP (53 mg, 0.1 mmol, 10 equiv), and HOBt (13 mg, 0.1 mmol, 10 equiv) were added to the MMTr-removed CPG (**17**) beads, and 3 mL of DMF was poured over the beads. DIPEA (175 μL, 1.0 mmol) was then added, the tube was capped tightly, and the mixture was agitated for 12 h at room temperature. The solution was filtered off, and beads were washed with copious amounts of DMF, DCM, DMF, and finally with 1% TEA in DMF. The coupling reaction was repeated once more to increase the coupling yield, and the unreacted 5′-NH_2 sites were finally capped with Ac_2O/TEA.

(d) Coupling of Hoechst Acid 15. Compound **15** (12.8 mg, 25 μmol, 5 equiv), PyBOP (27 mg, 50 μmol, 10 equiv), and HOBt (6.6 mg, 50 μmol, 10 equiv) were added to the MMTr-removed CPG (**18** or **19**) beads. Then DMF (3 mL) and DIPEA (175 μL, 1.0 mmol) were added, the tube was capped tightly, and the mixture was agitated for 24 h at room temperature. The solution was filtered off, and beads were washed with copious amount of DMF and methanol, followed by DCM, and dried under vacuum. The beads were fluoresced under longwave UV, indicating the successful addition of Hoechst acid.

(e) Cleavage and Deprotection. The dried CPG beads of **20** or **21** were transferred to a vial, and 0.1 M NaOH solution in 4:1 methanol/water (5 mL) was poured over the beads. The vial was capped tightly, and the mixture was agitated at room temperature for 1 h. The supernatant solution was pipetted out and desalted using NAP-10 (Sephadex G25) columns and HPLC grade water. The solution was diluted with 0.1% TFA in water (1 mL) and purified on reverse-phase HPLC using 0.1% TFA in water and gradient of acetonitrile (5 → 80% over 30 min). Both products **2** and **3** were eluted as broad peaks at ∼14 min.

Acknowledgment. This research work was supported by a grant (5R37DK09171-39) from the National Institutes of Health. We acknowledge valuable conversations with Hemavathi Challa and Istvan Szabo.

Supporting Information Available: Experimental details of **4**, figures showing ESI/TOF+ mass spectra of DNG conjugates **1**−**3**, UV spectrum of **3** and **15**, and temperature vs fluorescence emission change of DNA·DNG−H duplex (PDF). This material is available free of charge via the Internet at http://pubs.acs.org.

JA031557S